

Kinetics, Mechanism, and Spectroscopy of the Reversible Binding of Nitric Oxide to Aqueated Iron(II). An Undergraduate Text Book Reaction Revisited

Alicja Wanat,^{†,‡} Thorsten Schnepfensieper,[†] Grażyna Stochel,^{*,‡} Rudi van Eldik,^{*,†} Eckhard Bill,[§] and Karl Wieghardt[§]

Institute for Inorganic Chemistry, University of Erlangen-Nürnberg, Egerlandstrasse 1, 91058 Erlangen, Germany, Department of Inorganic Chemistry, Jagiellonian University, Ingardena 3, 30-060 Krakow, Poland, and Max-Planck-Institut für Strahlenchemie, Stiftstrasse 34-36, 45470 Mülheim an der Ruhr, Germany

Received June 13, 2001

A detailed kinetic and mechanistic analysis of the classical "brown-ring" reaction of $[\text{Fe}(\text{H}_2\text{O})_6]^{2+}$ with NO was performed using stopped-flow and laser flash photolysis techniques at ambient and high pressure. The kinetic parameters for the "on" and "off" reactions at 25 °C were found to be $k_{\text{on}} = 1.42 \times 10^6 \text{ M}^{-1} \text{ s}^{-1}$, $\Delta H_{\text{on}}^\ddagger = 37.1 \pm 0.5 \text{ kJ mol}^{-1}$, $\Delta S_{\text{on}}^\ddagger = -3 \pm 2 \text{ J K}^{-1} \text{ mol}^{-1}$, $\Delta V_{\text{on}}^\ddagger = +6.1 \pm 0.4 \text{ cm}^3 \text{ mol}^{-1}$, and $k_{\text{off}} = 3240 \pm 750 \text{ s}^{-1}$, $\Delta H_{\text{off}}^\ddagger = 48.4 \pm 1.4 \text{ kJ mol}^{-1}$, $\Delta S_{\text{off}}^\ddagger = -15 \pm 5 \text{ J K}^{-1} \text{ mol}^{-1}$, $\Delta V_{\text{off}}^\ddagger = +1.3 \pm 0.2 \text{ cm}^3 \text{ mol}^{-1}$. These parameters suggest that both reactions follow an interchange dissociative (i_a) ligand substitution mechanism, which correlates well with the suggested mechanism for the water exchange reaction on $[\text{Fe}(\text{H}_2\text{O})_6]^{2+}$. In addition, Mössbauer spectroscopy and EPR measurements were performed on the reaction product $[\text{Fe}(\text{H}_2\text{O})_5(\text{NO})]^{2+}$. The Mössbauer and EPR parameters closely resemble those of the $\{\text{FeNO}\}^7$ units in any of the other well-characterized nitrosyl complexes. It is concluded that its electronic structure is best described by the presence of high-spin Fe^{III} antiferromagnetically coupled to NO^- ($S = 1$) yielding the observed spin quartet ground state ($S = 3/2$), i.e., $[\text{Fe}^{\text{III}}(\text{H}_2\text{O})_5(\text{NO}^-)]^{2+}$, and not $[\text{Fe}^{\text{I}}(\text{H}_2\text{O})_5(\text{NO}^+)]^{2+}$ as usually quoted in undergraduate text books.

Introduction

The reaction of nitric oxide (NO) with transition metal ions plays an important role in environmental and biological processes. This is partly related to the unique redox behavior of NO as a result of its radical character in the ground state. This results in the tendency of NO to bind to metal centers either as NO^+ or as NO^- , such as in metmyoglobin where the Fe^{III} center binds NO in the form of $\text{Fe}^{\text{II}}-\text{NO}^+$,¹ or in reduced vitamin B₁₂ where Co^{II} binds NO in the form of $\text{Co}^{\text{III}}-\text{NO}^-$,² respectively. Such interactions demonstrate the biological importance of NO, which was announced "molecule of the year" in 1992.³

During undergraduate training in chemistry, the interaction of NO with aqueated Fe^{2+} is a reaction used as a spot test (brown ring test) for nitrate in introductory freshman laboratory courses. The details of the underlying reaction mechanism, with respect to the processes involved in the formation of the characteristic green-brown color of the $\text{Fe}^{\text{II}}-\text{NO}$ species, have not been well understood in the past. We have in recent work concentrated on the interaction of NO with a series of polyaminocarboxylate complexes of Fe^{II} as efficient scavengers for NO in the treatment of gaseous effluents of power plants.^{4,5} In these reactions, NO is reversibly bound by Fe^{II} complexes in aqueous solution according to the overall reaction given in eq 1. The displacement of coordinated water on $\text{Fe}^{\text{II}}(\text{L})$ is characterized

* Authors to whom correspondence should be addressed. E-mail: vaneldik@chemie.uni-erlangen.de (R.v.E.); stochel@chemia.uj.edu.pl (G.S.).

[†] University of Erlangen-Nürnberg.

[‡] Jagiellonian University.

[§] Max-Planck-Institut für Strahlenchemie.

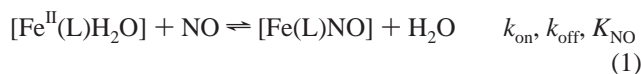
(1) Laverman, L. E.; Wanat, A.; Oszejca, J.; Stochel, G.; Ford, P. C.; van Eldik, R. *J. Am. Chem. Soc.* **2001**, *123*, 285.

(2) Wolak, M.; Stochel, G.; Zahl, A.; Schnepfensieper, T.; van Eldik, R. *J. Am. Chem. Soc.* **2001**, *123*, 9780.

(3) Culotta, E.; Koshland, D. E., Jr. *Science* **1992**, *258*, 1862.

(4) Schnepfensieper, T.; Finkler, S.; Czap, A.; van Eldik, R.; Heus, M.; Nieuwenhuizen, P.; Wreesmann, C.; Abma, W. *Eur. J. Inorg. Chem.* **2001**, 491.

(5) Schnepfensieper, T.; Wanat, A.; Stochel, G.; Goldstein, S.; Meyerstein, D.; van Eldik, R. *Eur. J. Inorg. Chem.* **2001**, 2317.



by the rate constant k_{on} , whereas the reverse displacement of coordinated NO by water is characterized by the rate constant k_{off} . The overall binding constant K_{NO} represents the ratio of the rate constants for the “on” and “off” reactions, i.e., $K_{\text{NO}} = k_{\text{on}}/k_{\text{off}}$. In our studies, a systematic variation of L resulted in K_{NO} values that varied between 1×10^2 (in the absence of L) and $1 \times 10^6 \text{ M}^{-1}$ (for chelates such as edta^{4-} and hedtra^{3-}). The tendency of $\text{Fe}^{\text{II}}(\text{L})$ to reversibly bind NO correlated directly with the oxygen sensitivity of the Fe^{II} complexes, suggesting that $\text{Fe}(\text{L})\text{NO}$ is stabilized in the form of $\text{Fe}^{\text{III}}(\text{L})(\text{NO}^-)$ similar to that found for the binding of dioxygen, viz., $\text{Fe}^{\text{III}}(\text{L})(\text{O}_2^-)$. These studies^{4,5} and the determination of the kinetic activation parameters⁶ have assisted the clarification of the underlying reaction mechanisms at a molecular level.

In the absence of L, the reaction product is $[\text{Fe}^{\text{II}}(\text{H}_2\text{O})_5\text{NO}]^{2+}$, i.e., $\{\text{Fe}-\text{NO}\}^7$ which can formally be stabilized as either $[\text{Fe}^{\text{I}}(\text{H}_2\text{O})_5(\text{NO}^+)]^{2+}$ or $[\text{Fe}^{\text{III}}(\text{H}_2\text{O})_5(\text{NO}^-)]^{2+}$. The reversible reaction of aqueated Fe^{II} salts with NO has been the topic of numerous investigations dating back as far as the late 19th century. Since 1906, the first quantitative investigations dealing with the binding of NO to ferrous complexes, especially from the work by Manchot et al. and others, were published.⁷ Much work has also been done on the decomposition products of the brown-ring compounds in acidic, neutral, and alkaline solutions,⁸ which was reviewed by Tarte.⁹ Rather conflicting results concerning the binding mode of NO to the metal center coming from magnetic susceptibility, ESR, IR, Mössbauer and other measurements were published later, from which the reaction product was assigned to be $[\text{Fe}^{\text{I}}(\text{H}_2\text{O})_5(\text{NO}^+)]^{2+}$.¹⁰ However, recent spectroscopic studies on non-heme iron nitrosyl centers in proteins^{11–17} and inorganic complexes^{18–23} in conjunction

with sophisticated theoretical calculations provide compelling evidence that the $\{\text{FeNO}\}^7$ unit with spin quartet ground state ($S_t = 3/2$) in the structurally well characterized iron nitrosyl complexes is best described by a bonding model based on high-spin Fe^{III} antiferromagnetically coupled to NO^- ($S = 1$). The conclusion is based on a vast body of consistent data derived from EXAFS and XAS Fe-edge measurements, absorption and MCD spectroscopy, resonance Raman spectroscopy, EPR and magnetic susceptibility measurements, and applied-field Mössbauer investigations on complete series of isostructural complexes containing the $\{\text{FeNO}\}^{6/7/8}$ motif.^{22,23} A number of reviews on the reactivity of this complex, and NO chemistry in general, have been published.²⁴

The kinetics of the complex-formation reaction using T-Jump techniques was reported by Chang et al.²⁵ and Weinstock et al.²⁶ with $k_{\text{on}} = 7.1 \times 10^5 \text{ M}^{-1} \text{ s}^{-1}$, $k_{\text{off}} = 1.5 \times 10^3 \text{ s}^{-1}$,¹¹ and $k_{\text{on}} = 6.2 \times 10^5 \text{ M}^{-1} \text{ s}^{-1}$, $k_{\text{off}} = 1.4 \times 10^3 \text{ s}^{-1}$ at 25 °C, respectively. The equilibrium constant, determined from the kinetic data resulted in $K_{\text{NO}} = k_{\text{on}}/k_{\text{off}} = 470$ and 450 M^{-1} , respectively. The accuracy of these parameters could recently be confirmed by using flash-photolysis techniques, resulting in somewhat higher values for the “on” and “off” reactions, with $k_{\text{on}} = 1.6 \times 10^6 \text{ M}^{-1} \text{ s}^{-1}$ and $k_{\text{off}} = 3.2 \times 10^3 \text{ s}^{-1}$ at 25 °C, which results in a K_{NO} value of $500 \pm 140 \text{ M}^{-1}$.⁵ The equilibrium constant measured directly with the aid of an NO sensitive electrode is slightly higher than the values obtained from the kinetic investigations, viz., $K_{\text{NO}} = 1.2 \times 10^3 \text{ M}^{-1}$ at 25 °C.⁴ Although the rate constants for the “on” and “off” reactions are known, no mechanistic conclusions could be drawn from these data due to the absence of the corresponding activation parameters (ΔH^\ddagger , ΔS^\ddagger , and ΔV^\ddagger) for these reactions.

In this paper we present a complete kinetic and mechanistic analysis of this classical reaction. The employed kinetic techniques enable detailed insight into the nature of the

- (6) Schnepfensieper, T.; Wanat, A.; Stochel, G.; Zahl, A.; van Eldik, R. Manuscript in preparation.
- (7) (a) Manchot, W.; Zechentmayer, K. *Annalen* **1906**, 350, 368. (b) Manchot, W. *Annalen* **1910**, 372, 179. (c) Manchot, W. *Ber. Dtsch. Chem. Ges.* **1914**, 47, 1601. (d) Schlesinger, H. I.; van Valkenburgh, H. B. *J. Am. Chem. Soc.* **1929**, 51, 1323 and literature cited therein.
- (8) (a) Dunstan; Dymond. *J. Chem. Soc.* **1887**, 51, 646. (b) Usher. *Z. Phys. Chem.* **1908**, 62, 622. (c) Divers; Hager. *J. Chem. Soc.* **1885**, 47, 361. (d) Huffner. *Z. Phys. Chem.* **1907**, 59, 416. (e) Kohlschutter; Sazanoff. *Ber. Dtsch. Chem. Ges.* **1911**, 44, 1423.
- (9) Tarte, E. *J. Ind. Chim. Belge* **1952**, 17, 42.
- (10) (a) Gray, H. B.; Bernal, I.; Billig, E. *J. Am. Chem. Soc.* **1962**, 84, 3404. (b) Griffith, W. P.; Lewis, J.; Wilkinson, G. *J. Chem. Soc.* **1958**, 3993. (c) Ogura, K.; Watanabe, M. *J. Inorg. Nucl. Chem.* **1981**, 43, 1239. (d) Burlamacchi, L.; Martini, G.; Tiezzi, E. *Inorg. Chem.* **1969**, 8, 2021. (e) Mosbæk, H.; Poulsen, K. G. *Acta Chem. Scand.* **1971**, 25, 2421.
- (11) Arciero, D. M.; Lipscomb, J. D.; Huynh B. H.; Kent, T. A.; Münck, E. *J. Biol. Chem.* **1983**, 258, 14981.
- (12) Nocek, J. M.; Kurtz, D. M., Jr.; Sage, J. T.; Xia, Y.-M.; Debrunner, P.; Shiemke, A. K.; Sanders-Loehr, T. M. *Biochemistry* **1988**, 27, 1014.
- (13) Rodriguez, J. H.; Xia, Y.-M.; Debrunner, P. *J. Am. Chem. Soc.* **1999**, 121, 7846.
- (14) Bill, E.; Bernhardt, F.-H.; Trautwein, A. X.; Winkler, H. *Eur. J. Biochem.* **1985**, 147, 177.
- (15) Haskin, C. J.; Ravi, N.; Lynch, J. B.; Münck, E.; Que, L., Jr. *Biochemistry* **1995**, 34, 11090.
- (16) Chen, V. J.; Orville, A. M.; Harpel, M. R.; Frolik, C. A.; Sureros, K. Münck, E.; Lipscomb, J. D. *J. Biol. Chem.* **1989**, 264, 21677.
- (17) Orville, A. M.; Chen, V. J.; Kriauciunas, A.; Harpel, M. R.; Fox, B. G.; Münck, E.; Lipscomb, J. D. *Biochemistry* **1992**, 31, 4602.
- (18) (a) Enemark, J. H.; Feltham, R. D. *Coord. Chem. Rev.* **1974**, 13, 339. (b) Feltham, R. D.; Enemark, J. H. In *Topic in Inorganic and Organometallic Stereochemistry*; Geoffroy, G. L., Ed.; Topics in Stereochemistry 12; Allinger, N. L.; Eliel, E. L., Series Eds.; Wiley: New York, 1981; p 155. (c) Westcott, B. L.; Enemark, J. H. In *Inorganic Electronic Structure and Spectroscopy*; Solomon, E. I., Lever, A. B. P., Eds.; Wiley: New York, 1999; Vol. II, p 403.
- (19) Wells, F. V.; McCann, S. W.; Wickman, H. H.; Kessel, S. L.; Hendrickson, D. N.; Feltham, R. D. *Inorg. Chem.* **1982**, 21, 2306.
- (20) Feig, A.; Bantista, M. T.; Lippard, S. J. *Inorg. Chem.* **1996**, 35, 6892.
- (21) Pohl, K.; Wieghardt, K.; Nuber, B.; Weiss, J. *J. Chem. Soc., Dalton Trans.* **1987**, 187.
- (22) (a) Brown, C. A.; Pavlosky, M. A.; Westre, T. E.; Zhang, Y.; Hedman, B.; Hodgson, K. O.; Solomon, E. I. *J. Am. Chem. Soc.* **1995**, 117, 715. (b) Westre, T. E.; Di Cicco, A.; Filipponi, A.; Natoli, C. R.; Hedman, B.; Solomon, E. I.; Hodgson, K. O. *J. Am. Chem. Soc.* **1994**, 116, 6757.
- (23) Hauser, C.; Glaser, T.; Bill, E.; Weyhermüller, T.; Wieghardt, K. *J. Am. Chem. Soc.* **2000**, 122, 4352.
- (24) (a) McCleverty, J. A. *Chem. Rev.* **1979**, 79, 53. (b) Connelly, N. G. *Inorg. Chim. Acta, Rev.* **1972**, 47. (c) Caulton, K. G. *Coord. Chem. Rev.* **1975**, 14, 317. (d) Bottomley, F. *Acc. Chem. Res.* **1978**, 11, 158. (e) Johnson, B. F. G.; McCleverty, J. A. *Prog. Inorg. Chem.* **1966**, 7, 277. (f) Feilisch, M.; Stamler, J. S. *Methods in Nitric Oxide Research*; John Wiley & Sons: Chichester, 1996.
- (25) Littlejohn, D.; Chang, S. G. *J. Phys. Chem.* **1982**, 86, 537.
- (26) Kustin, K.; Taub, I. A.; Weinstock, E. *Inorg. Chem.* **1966**, 5, 1079.

underlying reaction mechanism and a correlation with the lability and exchange mechanism of coordinated water in aquated Fe^{II} .²⁷ In addition, Mössbauer spectroscopy and EPR measurements were performed on the reaction product $\{\text{Fe}-\text{NO}\}^7$ and allow us to unequivocally resolve the discrepancy in the literature concerning the bonding character of this product.

Experimental Section

Materials. All chemicals were of analytical grade and used as received. Solutions were prepared with distilled and purified water using a Milli-Q water purification system. The stock solution of nitric oxide was prepared by degassing 0.2 M acetate buffer solution (pH 5.0) and then saturating it with NO. NO gas was purchased from Linde 93 or Riessner Gase in purity of at least 99.5 vol % and cleaned from traces of higher nitrogen oxides like N_2O_3 and NO_2 by passing through an Ascarite II column (NaOH on silica gel, Sigma-Aldrich) via vacuum line techniques. Dilutions of known concentration were prepared from this saturated solution. All experiments were performed under strict exclusion of air oxygen. Buffer solutions were deaerated for extended periods (in general 1 min per mL solution) with pure N_2 or Ar, before they were brought in contact with Fe^{II} salt ($\text{Fe}^{\text{II}}\text{SO}_4 \cdot 7\text{H}_2\text{O}$) or nitric oxide.

Measurements. pH measurements were performed on a Metrohm 623 pH meter with a Sigma glass electrode or on a Mettler Delta 340 pH meter. The concentration of free nitric oxide in solution was determined with an ISO-NOP electrode connected to an ISO-NO Mark II nitric oxide sensor from World Precision Instruments. The NO electrode consists of a membrane-covered anode which selectively oxidizes NO to NO_3^- ions. The resulting current is proportional to the concentration of NO in solution. The NO electrode was calibrated daily with fresh solutions of sodium nitrite and potassium iodide according to the method suggested by the manufacturers. The calibration factor ($\text{nA}/\mu\text{M}$) was determined with a linear fit program. The determination of the stability constant K_{NO} was performed as described before.⁴

UV/vis spectra were recorded on a Shimadzu UV-2100 spectrophotometer equipped with a thermostated cell compartment CPS-260. IR spectra were recorded with the use of a two-mirror ATR cell on an ATI Mattson FTIR Infinity spectrophotometer. The reflection instrument utilizes a Ge crystal as an internal reflection plate with a size of $50 \times 20 \times 2$ mm and 45° angle of incidence. For the $\{\text{Fe}-\text{NO}\}^7$ complex, four independent measurements of 100 scans were performed under inert gas atmosphere.

Mössbauer data were recorded on an alternating constant-acceleration spectrometer. The minimum experimental line width was 0.24 mm s^{-1} (full width at half-height). The sample temperature was maintained constant in an Oxford Instruments Variox cryostat; the $^{57}\text{Co}/\text{Rh}$ source (1.8 GBq) was kept at room temperature. Isomer shifts are quoted relative to iron metal at 300 K. X-band EPR spectra were recorded on a Bruker ELEXSYS E500 spectrometer equipped with a helium flow cryostat (Oxford Instruments ESR 910), an NMR gaussmeter, and a Hewlett-Packard frequency counter. The solution spectra were simulated with the program GFIT of the ESIM package (by E.B.). The powder simulation procedure uses effective g values for effective spin $S = 1/2$ and either anisotropic field-constant line widths or isotropic frequency-constant line widths.

The kinetics of NO release from $[\text{Fe}(\text{H}_2\text{O})_5\text{NO}]^{2+}$ was studied on a thermostated ($\pm 0.1^\circ\text{C}$) stopped-flow spectrometer (SX-

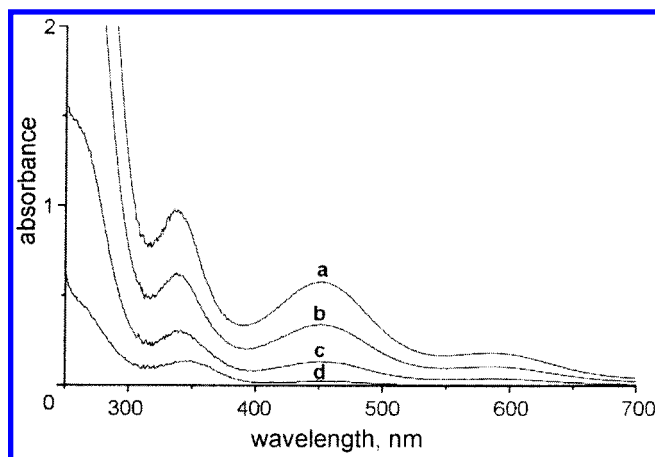


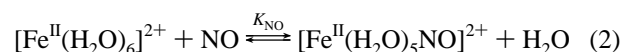
Figure 1. Absorption spectral changes recorded for the reaction of $3 \times 10^{-3} \text{ M } [\text{Fe}^{\text{II}}(\text{H}_2\text{O})_6]^{2+}$ with NO. Experimental conditions: 0.2 M acetate buffer, pH = 5.0, 25°C . Curves: trace a, $[\text{Fe}^{\text{II}}(\text{H}_2\text{O})_6]^{2+}$ solution saturated with NO; trace b, a + Ar brief (10 s); trace c, b + Ar brief (10 s); trace d, c + Ar brief (10 s).

18.MV, Applied Photophysics) coupled to an online data acquisition system. The changes in absorbance were monitored at 451 nm. The reported rate constants represent the mean values from at least five kinetic runs.

Laser flash photolysis kinetic studies were carried out with the use of the LKS.60 spectrometer from Applied Photophysics for detection and a Nd:YAG laser (SURLITE I—10 Continuum) pump source operating in the second ($\lambda_{\text{exc}} = 532 \text{ nm}$) harmonic (245 mJ pulses with $\sim 7 \text{ ns}$ pulse width). Spectral changes at 451 nm were monitored using a 100 W xenon arc lamp, monochromator, and photomultiplier tube PMT—1P22. The absorbance reading was balanced to zero before the flash, and data were recorded on a digital storage oscilloscope DSO HP 54522A and then transferred to a computer for subsequent analysis. Gastight quartz cuvettes and a pill-box cell combined with high-pressure equipment²⁸ were used at ambient and under high pressure (up to 170 MPa), respectively. At least 30 kinetic runs were recorded under all conditions, and the reported rate constants represent the mean values of these.

Results and Discussion

Spectroscopic Observations. The UV/vis spectrum of $[\text{Fe}^{\text{II}}(\text{H}_2\text{O})_6]^{2+}$ measured in 0.2 M acetate buffer solution at pH = 5.0 exhibits no absorption band between 250 and 800 nm. As can be seen from Figure 1, exposure of a degassed solution of $[\text{Fe}^{\text{II}}(\text{H}_2\text{O})_6]^{2+}$ to excess NO leads to a significant increase in absorbance giving band maxima at 336 ($\epsilon = 440$), 451 ($\epsilon = 265$), and 585 nm ($\epsilon = 85 \text{ M}^{-1} \text{ cm}^{-1}$). Upon removal of NO from solution with a stream of Ar gas, the spectral changes were completely reversed, indicating that the following equilibrium (eq 2) must be valid under the selected conditions.



Using UV/vis spectroscopy combined with the electrochemical detection of NO, the equilibrium constant K was determined to be $(1.15 \pm 0.05) \times 10^3 \text{ M}^{-1}$ in 0.1 M acetate buffer, pH = 5.0 and 23°C .

(27) (a) Swift, T. J.; Connick, R. E. *J. Chem. Phys.* **1962**, *37*, 307. (b) Ducommun, Y.; Newman, K. E.; Merbach, A. E. *Inorg. Chem.* **1980**, *19*, 3696.

(28) Spitzer, M.; Gartig, F.; van Eldik, R. *Rev. Sci. Instrum.* **1988**, *59*, 2092.

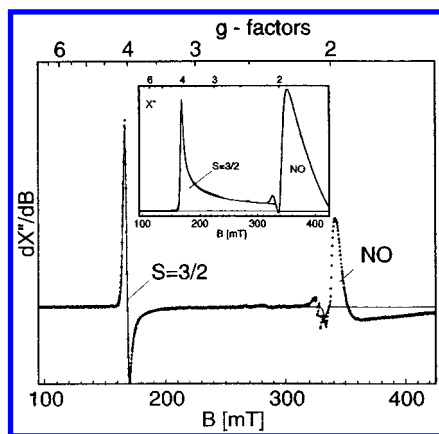


Figure 2. Experimental and simulated X-band EPR derivative spectra of $[\text{Fe}(\text{H}_2\text{O})_5(\text{NO})]^{2+}$ and numerical integrated spectrum (inset) with respective simulations. Experimental conditions: 0.1 mM Fe^{II} solution saturated with NO at 298 K (the sample was an aliquot of the Mössbauer preparation); measuring temperature 10 K, microwave frequency 9.4625 GHz, power 100 μW , modulation 1.2 mT at 100 kHz. The simulation (trace “ $S = 3/2$ ”) was obtained with effective g values $g = (4.04, 4.04, 2.0)$ and constant isotropic line width $W = 5$ mT (Gaussian).

IR spectroscopy is considered to be a useful tool for the determination of the binding mode and oxidation state of NO in metal-based complexes.^{24a,29} The ATR-IR spectrum was measured with a 0.2 M unbuffered solution ($\text{pH} = 3.1$) of $[\text{Fe}^{\text{II}}(\text{H}_2\text{O})_6]^{2+}$ saturated with NO. The formation of a single peak at 1810 cm^{-1} was observed, indicating the formation of $[\text{Fe}^{\text{II}}(\text{H}_2\text{O})_5\text{NO}]^{2+}$. Taking into account that for the $\text{Fe}^{\text{II}}(\text{L})\text{NO}$ complexes ($\text{L} = \text{polyaminocarboxylate}$) the observed wavenumbers are found to be around 1777 cm^{-1} ($\text{L} = \text{edta}^{4-}$), which are known to bind NO as $\text{Fe}^{\text{III}}-\text{NO}^-$,^{22a} the slightly shifted peak in $[\text{Fe}^{\text{II}}(\text{H}_2\text{O})_5\text{NO}]^{2+}$ should correspond to a species formally written as $[\text{Fe}^{\text{III}}(\text{H}_2\text{O})_5(\text{NO}^-)]$ with a charge contribution indicating a pronounced electron donation from the metal to the ligand.

The X-band EPR spectrum of the nitrosylated solution was measured in frozen state at 10 K as shown in Figure 2, from which the corresponding absorption spectrum was obtained by numerical integration of the experimental signals (inset). The appearance of two absorption maxima reveals that two major subspectra are present with similar abundances. The very asymmetric broad absorption centered at about $g = 1.9$ is typical of “free” NO molecules in frozen solution (not simulated). The low g value and the large width of this $S = 1/2$ spectrum indicate the presence of substantial spin–orbit interaction, as expected for the NO radical. The low-field part of the experimental spectrum, however, could be readily simulated by adopting an independent subspectrum with effective g values $g = (4.04, 4.04, 2.0)$, which are typical of a spin quartet species (trace “ $S = 3/2$ ”) with dominating zero-field splitting, $D \gg h\nu$ (0.3 cm^{-1} at X-band), and vanishing rhombicity, $E/D = 0$. Similar spectra have been observed for solutions of $[\text{Fe}(\text{edta})(\text{NO})]^{2-}$ or $[(1,4,7\text{-trimethyl-1,4,7-triazacyclononane})\text{Fe}(\text{NO})(\text{N}_3)_2]$.²³ Hence, the subspectrum can be assigned to the nitrosylated iron–aqua complex and it proves the $S = 3/2$ ground state of the $\{\text{FeNO}\}^7$ core. We mention that residual precursor high-spin Fe^{II} ions in water

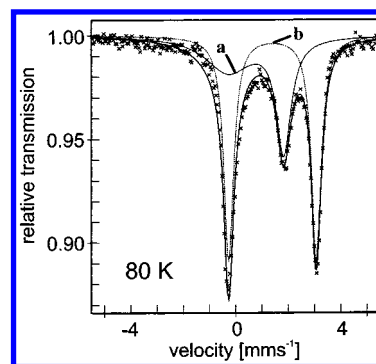


Figure 3. Zero-field Mössbauer spectrum of $[\text{Fe}(\text{H}_2\text{O})_5(\text{NO})]^{2+}$ (0.2 M Fe^{II} solution saturated with NO at 298 K) at 80 K. The bold solid line is the result of a fit with two Lorentzian doublets to the experimental (\times) data (thin line “a”, $\{\text{FeNO}\}^7$; thin line “b”, residual Fe^{II}).

($S = 2$) are virtually EPR silent at the selected experimental conditions, due to the presence of extremely broad spectra induced by the large zero-field splitting of the integer-spin species.

The zero-field Mössbauer spectrum of the ^{57}Fe -enriched nitrosylated iron solution measured at 80 K shows three lines which can be deconvoluted into two overlapping quadrupole doublets with an intensity ratio of about 2:3 (Figure 3). The major doublet shows a very large isomer shift, $d = 1.39$ mm s^{-1} , and a large quadrupole splitting, $\Delta E_Q = 3.33$ mm s^{-1} , like the precursor $\text{Fe}^{\text{II}}\text{SO}_4(\text{aq})$. Hence, the contribution (58%) can be assigned to nonreacted $[\text{Fe}^{\text{II}}(\text{H}_2\text{O})_6]^{2+}$, which perfectly agrees with that expected for a saturated NO solution and the K_{NO} value given above. The formation of the nitrosyl complex is indicated by the appearance of the resolved peak at about 1.8 mm s^{-1} . The corresponding subspectrum was successfully simulated by adopting an asymmetric Lorentzian doublet with identical line intensities but significantly different line widths. The related Mössbauer parameters, $d = 0.76$ mm s^{-1} , $\Delta E_Q = 2.1$ mm s^{-1} , are practically identical with those previously reported for $\text{Fe}(\text{NO})\text{SO}_4(\text{aq})$, $d = 0.76$ mm s^{-1} , $\Delta E_Q = 2.3$ mm s^{-1} .^{10e,30} We presume that the line asymmetry and broadening at 80 K owes its origin to the onset of spin relaxation with rates intermediate to the nuclear Larmor precession and the lifetime. The assignment of lines applied in the Lorentzian fit shown in Figure 3 and validity of the obtained parameters were confirmed from a measurement at liquid helium temperature (not shown). Since the Mössbauer and EPR parameters of the $[\text{Fe}(\text{H}_2\text{O})_5(\text{NO})]^{2+}$ complex closely resemble those of the $\{\text{FeNO}\}^7$ units in any of the other well-characterized nitrosyl complexes, we infer that its electronic structure is also best described by the presence of high-spin Fe^{III} antiferromagnetically coupled to NO^- ($S = 1$) yielding the observed spin quartet ground state ($S = 3/2$).

Flash-Photolysis Kinetics. The rates of NO binding to $\text{Fe}^{\text{II}}(\text{L})$ complexes (where $\text{L} = \text{H}_2\text{O}$, polyaminocarboxylates) are convenient to measure by flash photolysis, which can be employed to study the kinetics of reactions on a significantly faster time scale than stopped-flow technique.

(30) The isomer shifts reported in ref 10e, which are given with respect to sodium nitroprusside, were converted to values relative to α -iron at ambient temperature by subtracting 0.258 mm s^{-1} .

(29) Mingos, D. M. P.; Sherman, D. J. *Adv. Inorg. Chem.* **1989**, *34*, 293.

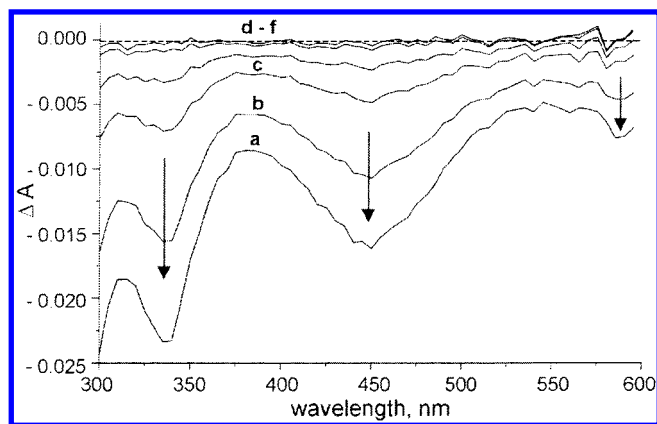
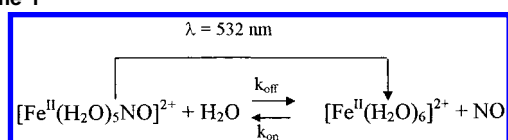


Figure 4. Transient absorption difference spectra for $[\text{Fe}(\text{H}_2\text{O})_5\text{NO}]^{2+}$ after laser flash photolysis at 532 nm. Experimental conditions: $[\text{Fe}(\text{H}_2\text{O})_6^{2+}] = 0.012 \text{ M}$, $[\text{NO}] = 3.6 \times 10^{-4} \text{ M}$, 0.2 M acetate buffer, pH = 5.0, 22 °C. Curves: a, after 25 μs ; b, after 50 μs ; c, after 100 μs ; d, after 150 μs ; e, after 250 μs ; f, after 450 μs .

Scheme 1



Irradiation at 532 nm induces dissociation of the nitrosyl complex and rapid release of NO, followed by relaxation of the system back to the original equilibrium position (Scheme 1).

As can be seen from Figure 4, 532 nm flash photolysis of $[\text{Fe}^{\text{II}}(\text{H}_2\text{O})_5\text{NO}]^{2+}$ in 0.2 M acetate buffer solution at pH = 5 results in spectral changes which are described by prompt transient bleaching with the largest change in absorbance centered at 336, 451, and 585 nm. This is consistent with the photolabilization of NO from $[\text{Fe}^{\text{II}}(\text{H}_2\text{O})_5\text{NO}]^{2+}$ and formation of free NO and $[\text{Fe}^{\text{II}}(\text{H}_2\text{O})_6]^{2+}$. After a delay of 450 μs , the transient bleaching disappears and the spectrum returns to the baseline ascribed to the regeneration of the original nitrosyl complex. The decay of the transient bleaching was followed using single-wavelength detection at 451 nm and could be analyzed as a one-exponential decay as shown in Figure S1 (Supporting Information). As can be seen, the rebinding of NO to $[\text{Fe}^{\text{II}}(\text{H}_2\text{O})_6]^{2+}$ is completed within 0.2 ms at $[\text{Fe}^{\text{II}}(\text{H}_2\text{O})_6^{2+}] = 0.018 \text{ M}$ and 25 °C for which $k_{\text{obs}} = 3.0 \times 10^4 \text{ s}^{-1}$.

The rate of the reaction approaching equilibrium with one of the components (in our case $[\text{Fe}^{\text{II}}(\text{H}_2\text{O})_6]^{2+}$) in large excess is expected to follow pseudo-first-order kinetics to give a rate constant k_{obs} expressed by eq 3. Accordingly, plots of

$$k_{\text{obs}} = k_{\text{on}}[\text{Fe}^{\text{II}}(\text{H}_2\text{O})_6^{2+}] + k_{\text{off}} \quad (3)$$

k_{obs} vs $[\text{Fe}^{\text{II}}(\text{H}_2\text{O})_6^{2+}]$ should be linear with slopes equal to k_{on} and intercepts equal to k_{off} . In the studied system the equilibrium constant K_{NO} is sufficiently small that extrapolation to $[\text{Fe}^{\text{II}}(\text{H}_2\text{O})_6^{2+}] = 0$ gives a measurable intercept, i.e., k_{off} . However, such intercepts are subjected to extrapolation errors. All kinetic experiments were performed in 0.2 M acetate buffer at pH = 5.0 with at least a 10-fold excess of $[\text{Fe}^{\text{II}}(\text{H}_2\text{O})_6]^{2+}$ using laser irradiation at $\lambda_{\text{irr}} = 532 \text{ nm}$.

Table 1. Rate Constants and Activation Parameters for the Reversible Binding of NO to $[\text{Fe}^{\text{II}}(\text{H}_2\text{O})_6]^{2+}$ ^a

temp (°C)	pressure (MPa)	$k_{\text{on}} (\text{M}^{-1} \text{s}^{-1})$	$k_{\text{off}} (\text{s}^{-1})$
5	0.1	$(4.4 \pm 0.2) \times 10^5$	760 ± 380
10		$(6.2 \pm 0.2) \times 10^5$	1170 ± 380
15		$(8.1 \pm 0.1) \times 10^5$	1690 ± 290
20		$(1.06 \pm 0.10) \times 10^6$	2380 ± 220
25		$(1.42 \pm 0.04) \times 10^6$	3240 ± 750
30		$(1.86 \pm 0.03) \times 10^6$	4420 ± 590
35		$(2.31 \pm 0.05) \times 10^6$	7050 ± 900
20	10	$(1.04 \pm 0.04) \times 10^6$	2190 ± 650
	50	$(9.27 \pm 0.06) \times 10^5$	2120 ± 100
	90	$(8.15 \pm 0.24) \times 10^5$	2060 ± 470
	130	$(7.55 \pm 0.12) \times 10^5$	2050 ± 240
	170	$(6.97 \pm 0.14) \times 10^5$	2000 ± 290
$\Delta H^\ddagger (\text{kJ/mol})$		37.1 ± 0.5	48.4 ± 1.4
$\Delta S^\ddagger (\text{J/(K mol)})$		-3.3 ± 2.0	-15.3 ± 4.7
$\Delta V^\ddagger (\text{cm}^3/\text{mol})$		$+6.1 \pm 0.4$	$+1.3 \pm 0.2$

^a Experimental conditions: 0.2 M acetate buffer, pH = 5.0, $[\text{NO}] = 3.6 \times 10^{-4} \text{ M}$, $[\text{Fe}^{\text{II}}(\text{H}_2\text{O})_6^{2+}] = 0.006\text{--}0.03 \text{ M}$, $\lambda_{\text{irr}} = 532 \text{ nm}$, $\lambda_{\text{detect}} = 451 \text{ nm}$.

In agreement with eq 3, plots of k_{obs} vs $[\text{Fe}^{\text{II}}(\text{H}_2\text{O})_6^{2+}]$ are linear with nonzero intercepts as displayed in Figure S2 (Supporting Information) for the temperature range 5–35 °C. The k_{on} and k_{off} values determined from these plots (Table 1) at 25 °C were used to estimate the overall equilibrium constant K for reaction 2, which resulted in $K = k_{\text{on}}/k_{\text{off}} = 440 \pm 110 \text{ M}^{-1}$. This value is in reasonable agreement with the thermodynamically determined value reported above; the deviations are most probably related to errors involved in the determination of k_{off} via extrapolation of the kinetic data obtained in the flash-photolysis experiments. The value of K was also calculated ($k_{\text{on}}/k_{\text{off}}$) for the other temperatures, from which it follows that K decreases with increasing temperature, i.e., reaction 2 is an exothermic process with $\Delta H^\circ = -11.4 \pm 1.8 \text{ kJ mol}^{-1}$ and $\Delta S^\circ = +12 \pm 6 \text{ J K}^{-1} \text{ mol}^{-1}$.

The temperature dependence of k_{on} and k_{off} (Table 1) was used to construct linear Eyring plots (Figure S3, Supporting Information), from which the activation parameters ΔH^\ddagger and ΔS^\ddagger were determined. The values for k_{on} are $\Delta H^\ddagger_{\text{on}} = 37.1 \pm 0.5 \text{ kJ mol}^{-1}$ and $\Delta S^\ddagger_{\text{on}} = -3 \pm 2 \text{ J K}^{-1} \text{ mol}^{-1}$; for k_{off} these are $\Delta H^\ddagger_{\text{off}} = 48.4 \pm 1.4 \text{ kJ mol}^{-1}$ and $\Delta S^\ddagger_{\text{off}} = -15 \pm 5 \text{ J K}^{-1} \text{ mol}^{-1}$. Since the k_{off} values are obtained by extrapolation of the k_{obs} vs $[\text{Fe}^{\text{II}}(\text{H}_2\text{O})_6^{2+}]$ plots and the determination of ΔS^\ddagger in principle involves an extrapolation to $1/T = 0$, it is reasonable to expect that the values of ΔS^\ddagger , especially for the “off” reaction, can be subjected to large error limits. Thus mechanistic conclusions based on the values reported for ΔS^\ddagger are difficult to reach, especially when they are close to 0.

A more reliable mechanistic discrimination parameter is the volume of activation ($\Delta V^\ddagger = -RT(\text{d} \ln k_i/\text{d}P)_T$, where k_i is the rate constant at a particular pressure)³¹ derived from the effect of hydrostatic pressure P on the kinetics of the reaction. The effect of pressure on the reaction of $[\text{Fe}^{\text{II}}(\text{H}_2\text{O})_6]^{2+}$ with NO was studied using a high-pressure flash-

(31) (a) van Eldik, R.; Asano, T.; le Noble, W. J. *Chem. Rev.* **1989**, *89*, 549–688. (b) van Eldik, R.; Dücker-Benfer, C.; Thaler, F. *Adv. Inorg. Chem.* **2000**, *49*, 1.

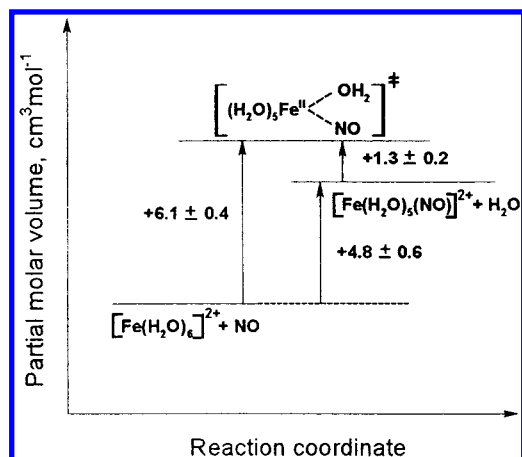


Figure 5. Volume profile for reaction 2 based on the determined volumes of activation.

photolysis technique. The flash-photolysis experiments were carried out in 0.2 M acetate buffer solutions, at 20 °C and in the pressure range 0.1–170 MPa. The results are reported in Figure S4 (Supporting Information).

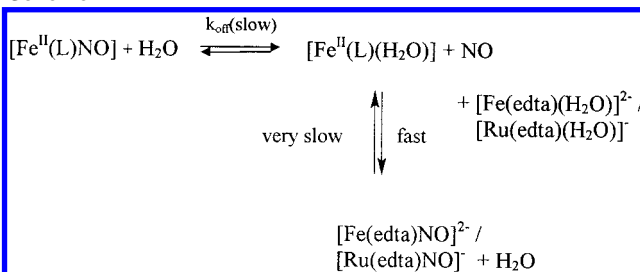
From plots of k_{obs} vs $[\text{Fe}^{\text{II}}(\text{H}_2\text{O})_6]^{2+}$ at different pressures, values of k_{on} and k_{off} were determined, and linear $\ln(k_i)$ vs pressure plots (Figure S5, Supporting Information) show that both rate constants decrease with increasing pressure, resulting in small positive volumes of activation, viz., $\Delta V_{\text{on}}^\ddagger = +6.1 \pm 0.4 \text{ cm}^3 \text{ mol}^{-1}$ and $\Delta V_{\text{off}}^\ddagger = +1.3 \pm 0.2 \text{ cm}^3 \text{ mol}^{-1}$ for the “on” and “off” reactions, respectively. The effect of pressure on the back reaction is rather small, resulting in almost the same, within the experimental error limits, k_{off} values at different pressures (Table 1). The reaction volume (ΔV) for the overall equilibrium ($\Delta V = \Delta V_{\text{on}}^\ddagger - \Delta V_{\text{off}}^\ddagger$) is $+4.8 \pm 0.6 \text{ cm}^3 \text{ mol}^{-1}$, indicating that there is an overall increase in partial molar volume during the displacement of coordinated water by NO. A volume profile constructed on the basis of these data is given in Figure 5, which suggests that reaction 2 proceeds according to a dissociative interchange mechanism (see further discussion).

Stopped-Flow Kinetics. Since the k_{off} values obtained from the $[\text{Fe}(\text{H}_2\text{O})_6]^{2+}$ concentration dependence of k_{obs} are subjected to extrapolation errors, it is important to confirm their reliability in a more direct way. As it was already shown,⁵ the most suitable method to measure k_{off} directly is to use an NO-trapping technique. In such a case the nitrosyl complex is treated with another complex that binds NO stronger and more rapidly than the system under investigation. When an excess of the trapping complex is employed, NO release from the nitrosyl complex becomes the rate-limiting step in the reaction sequence shown in Scheme 2, and k_{off} can be determined directly from the observed kinetic trace, viz., $k_{\text{obs}} = k_{\text{off}}$.

Two complexes can be employed as efficient NO scavengers in such trapping experiments, viz., $[\text{Fe}^{\text{II}}(\text{edta})(\text{H}_2\text{O})]^{2-}$ or $[\text{Ru}^{\text{III}}(\text{edta})(\text{H}_2\text{O})]^-$. Both of them react rapidly with NO (k_{on} is ca. $1 \times 10^8 \text{ M}^{-1} \text{ s}^{-1}$ at pH = 5.0 and 25 °C)⁵ to form the corresponding nitrosyl complexes.

In the studied reaction, $[\text{Fe}^{\text{II}}(\text{edta})(\text{H}_2\text{O})]^{2-}$ (in 20-fold excess) was used to trap nitric oxide released from $[\text{Fe}^{\text{II}}(\text{H}_2\text{O})_5\text{NO}]^{2+}$.

Scheme 2



$\text{NO}]^{2+}$. Spectral changes recorded for this reaction (see Figure S6, Supporting Information) are described by two clear shifts in the absorbance maxima from 451 to 435 nm and from 585 to 633 nm, indicating the decay of $[\text{Fe}^{\text{II}}(\text{H}_2\text{O})_5\text{NO}]^{2+}$ and formation of a new nitrosyl complex, viz., $[\text{Fe}^{\text{II}}(\text{edta})(\text{NO})]^{2-}$. In order to determine the k_{off} value, the reaction was studied using stopped-flow techniques. At room temperature the reaction occurs within the dead time of the apparatus; hence the rate measurements were performed at 5 °C. At this temperature a rapid increase in absorbance at 432 nm was observed and the reaction was complete within 10 ms with $k_{\text{obs}} = 788 \pm 50 \text{ s}^{-1}$. A typical stopped-flow trace for this reaction is shown in Figure S7 (Supporting Information). The observed rate constants were found to be independent of the concentration of the trapping complex and therefore represent the value for k_{off} . The value of k_{off} determined in this manner is consistent, within experimental error limits, with that obtained from extrapolating k_{obs} vs $[\text{Fe}^{\text{II}}(\text{H}_2\text{O})_6]^{2+}$ in the flash-photolysis experiments at 5 °C. It should be noted that the trapping technique employed enables a direct measurement of the dissociation rate constant and in principle must result in a more accurate value for k_{off} than that obtained using the indirect extrapolation method. However, the magnitude of k_{off} is such that stopped-flow techniques could not be used to measure this rate constant as a function of temperature and pressure.

Overall Reaction Mechanism. From the spectral (UV-vis, IR, Mössbauer, EPR) data reported for the nitrosyl reaction product, it is clear that the complex can be formulated as $[\text{Fe}^{\text{III}}(\text{H}_2\text{O})_5(\text{NO}^-)]^{2+}$ and not as $[\text{Fe}^{\text{I}}(\text{H}_2\text{O})_4(\text{NO}^+)]^{2+}$ as claimed before.¹⁰ This means that displacement of coordinated water on $[\text{Fe}^{\text{II}}(\text{H}_2\text{O})_6]^{2+}$ by NO results in the formal oxidation of Fe^{II} to Fe^{III} and the reduction of NO to NO^- . It is reasonable to expect that the “on” reaction will to some extent be related to the water exchange reaction on $[\text{Fe}^{\text{II}}(\text{H}_2\text{O})_6]^{2+}$, for which $k_{\text{ex}} = 4.4 \times 10^6 \text{ s}^{-1}$ at 25 °C, $\Delta H^\ddagger = 41.4 \text{ kJ mol}^{-1}$, $\Delta S^\ddagger = +21.2 \text{ J K}^{-1} \text{ mol}^{-1}$, and $\Delta V^\ddagger = +3.8 \text{ cm}^3 \text{ mol}^{-1}$,²⁷ in a way similar to that recently reported for the binding of NO to $[\text{Fe}^{\text{III}}(\text{TTPS})(\text{H}_2\text{O})_2]^{3-}$.³² The rate of water exchange is much faster than the “on” kinetics for the reaction with NO, and the values of ΔH^\ddagger are indeed very similar. In addition, the activation volumes reported for the water exchange process and the reaction with NO are also very similar and suggest that both reactions occur according to a dissociative interchange (I_d) mechanism.³¹ It follows that

(32) Schnepfensieper, T.; Zahl, A.; van Eldik, R. *Angew. Chem.* **2001**, *40*, 1678.

water exchange on $[\text{Fe}^{\text{II}}(\text{H}_2\text{O})_6]^{2+}$ controls not only the rate but also the nature of the mechanism for the binding of NO. This rate-determining displacement of coordinated water is followed by a rapid intramolecular charge-redistribution process to lead to the final $[\text{Fe}^{\text{III}}(\text{H}_2\text{O})_5(\text{NO}^-)]^{2+}$ product. During the “off” reaction, the release of NO will involve electron transfer to form $[\text{Fe}^{\text{II}}(\text{H}_2\text{O})_5\text{NO}]^{2+}$, followed by the displacement of NO by water. The latter step exhibits a much higher activation enthalpy than both the water exchange and “on” reactions, which must be related to the stronger Fe–NO bond and accounts for the significantly slower “off” reaction. As a result the overall reaction enthalpy for the binding of NO is $-11.4 \pm 1.8 \text{ kJ mol}^{-1}$, i.e., the process is exothermic, and K_{NO} decreases with increasing temperature. The activation volume for the “off” reaction is small positive and also in line with an interchange dissociative (I_d) ligand substitution mechanism. Alternatively, the release of NO from $\text{Fe}^{\text{III}}\text{--NO}^-$ in the “off” reaction can be visualized as a homolysis reaction that results in the formation of Fe^{II} and NO, in which bond cleavage is accompanied by formal reduction of Fe^{III} to Fe^{II} , and involves the simultaneous entry of a water molecule, i.e., a water-“assisted” homolysis reaction. The overall positive reaction volume of $+4.8 \pm 0.6 \text{ cm}^3 \text{ mol}^{-1}$ results from the displacement of a water by an NO molecule in the coordination sphere of Fe^{II} and is in agreement with the small positive value of $+12 \pm 6 \text{ J K}^{-1} \text{ mol}^{-1}$ found for ΔS° .

We conclude that the detailed spectroscopic and kinetic studies performed on the reaction of aquated Fe^{II} with NO has resolved the nature of the nitrosyl product and the mechanism of the “on” and “off” reactions. These are controlled by ligand substitution processes on the iron metal center. In addition, it is important to note that although NO is a radical, it behaves as a normal nucleophile during such ligand displacement reactions. Its radical nature, however, does require a formal charge transfer process to occur in order to stabilize the nitrosyl reaction product. It will now be appropriate to correct numerous undergraduate chemistry text books that incorrectly describe this “simple” reaction.

Acknowledgment. The authors gratefully acknowledge financial support from the Deutsche Forschungsgemeinschaft, the Max-Buchner-Forschungsstiftung, and DAAD (fellowship to A.W.). Studies at the Jagiellonian University were supported by the State Committee for Scientific Research, Poland, KBN (3TO9A11515 and 1605/T09/2000/19), and the Foundation for Polish Science (“Fastkin” No. 8/97).

Supporting Information Available: A total of seven figures in which UV–vis spectra, kinetic traces, and plots of k_{obs} as a function of concentration, temperature, and pressure are reported for the reversible binding of NO to aquated iron(II). This material is available free of charge via the Internet at <http://pubs.acs.org>.

IC010628Q